

# Supplementary Materials: A Semi-Analytic Model for Estimating Total Suspended Sediment Concentration in Turbid Coastal Waters of Northern Western Australia using MODIS-Aqua 250 m Data

Passang Dorji, Peter Fearn and Mark Broomhall

## 1. Comparison of Reflectance Models for Nechad, et al. [1] and SASM

The  $\omega'_b(\lambda)$  by definition can be used as a proxy for reflectance because it is a ratio of the amount of light backscattered to the amount of light absorbed by water and its constituents Nechad, Ruddick and Park [1], hereafter referred as NRP. Thus,  $\omega'_b(\lambda)$  from both the NRP and SASM model is used here for the comparative analysis using HydroLight-simulated data for different water types. From the HydroLight simulations, we generate  $r_{rs}$  for given IOP models representing different water types [2] to be inverted to compute  $\omega'_b(\lambda)$  for use in model comparisons between NRP and SASM derived estimates of  $\omega'_b(\lambda)$ . Each model derived  $\omega'_b(\lambda)$  is then validated using the true  $\omega'_b(\lambda)$  given by Equation (8). The true  $\omega'_b(\lambda)$  are calculated from the  $a(\lambda)$  and  $b_b(\lambda)$  we used as the inputs in the HydroLight simulation.

### 1.1. NRP Reflectance Model

The reflectance model used in the formulation of  $r_{rs}(\lambda)$  by NRP assumes  $r_{rs}(\lambda)$  is based on the first order approximation of Gordon, et al. (1988) [3]:

$$r_{rs}(\lambda) = \frac{f'}{Q} \frac{b_b(\lambda)}{a(\lambda) + b_b(\lambda)} = \frac{f'}{Q} \frac{\omega'_b(\lambda)}{1 + \omega'_b(\lambda)} \quad (S1)$$

where  $f'$  is a varying dimensionless factor described by Morel and Gentili (1991) [57] and  $Q$  is the ratio of subsurface upwelling irradiance to the subsurface upwelling radiance. The ratio of the total backscattering coefficient to total absorption coefficient ( $\omega'_b(\lambda)$ ) is related to subsurface remote sensing reflectance as follows:

$$\omega'_b(\lambda) = \frac{\rho_w(\lambda)}{\gamma - \rho_w(\lambda)} \quad (S2)$$

where  $\rho_w(\lambda) = \pi \Re r_{rs}(\lambda)$  and  $\gamma = \pi \Re r_{rs}(\lambda) f' / Q \approx 0.216$  with  $\Re = 0.529$  and  $f' / Q = 0.13$  (refer to [1] for details)

### 1.2. SASM Reflectance Model

SASM computes  $r_{rs}$  based on the second order approximation of Gordon, et al. [3] as shown in Equation (1) using coefficients  $g_1$  and  $g_2$  from Lee, et al. [4] optimized for turbid waters. In the SASM,  $r_{rs}(\lambda)$  is related to  $\omega'_b(\lambda)$  as follow:

$$\omega'_b(\lambda) = \frac{x(\lambda)}{1 - x(\lambda)} \quad (S3)$$

where  $x$  is given by Equation (15).

## 2. HydroLight Simulation

HydroLight 4.2 by Mobley was used to simulate case-2 water remote sensing reflectance for infinitely deep water using a four components model. The four components were: (1) pure water; (2)

pigmented particles or chlorophyll (CHL); (3) coloured dissolved organic matter (CDOM) and (4) mineral particles (TSS).

For all HydroLight simulations, the following details were kept unchanged: the phase function for component 1 was a Rayleigh-like phase function, components 2 and 4 used Petzold “average particle” phase functions, and component 3 used an isotropic phase function. Standard (IOP) models from HydroLight were used to compute components’ scattering and absorption coefficients: the component 1 absorption coefficient was from and the scattering coefficients were from [5]. The component 2 absorption coefficient for a chlorophyll-specific absorption was derived from and the scattering coefficient was computed using the [6] near surface power law model. The specific absorption for component 3 was computed using an exponential decay model and the component 4 specific absorption and scattering coefficients were from HydroLight data for Calcareous sand.

HydroLight simulations were performed for a solar zenith angle of 30°, wind speed of 5 m·s<sup>-1</sup>, and for a clear sky using Harrison and Coombes’ sky model for different TSS concentration, CHL concentration, and CDOM absorption. TSS concentration values ranged from 0–200 mg/L. For the range 0–50 mg/L the TSS concentration was increased at the rate of 0.2 mg/L and for the 50–200 mg/L range the rate of increment was 2.0 mg/L. The concentration of chlorophyll was set at 0.1 mg·m<sup>-3</sup>, 1 mg·m<sup>-3</sup>, 5 mg·m<sup>-3</sup> and 10 mg·m<sup>-3</sup> and CDOM absorption of 0.1 m<sup>-1</sup> and 1.0 m<sup>-1</sup> were used in the simulation. The combinations of CHL and CDOM were used to define 6 different water types, shown in Table S1.

**Table S1.** Six different water types grouped based on CHL concentration and CDOM absorption.

CHL (mg·m <sup>-3</sup> ) and CDOM (m <sup>-1</sup> )	Water Type
CHL 0.1 and CDOM 0.1	I
CHL 1.0 and CDOM 0.1	II
CHL 5.0 and CDOM 0.1	III
CHL 10.0 and CDOM 0.1	IV
CHL 0.1 and CDOM 1.0	V
CHL 10.0 and CDOM 1.0	VI

### 3. Reflectance Model Evaluation

We present  $\omega'_b(\lambda)$  modelled using Equations (22) and (23) for the 6 different water types as a function of TSS concentration, compared with HydroLight simulated  $\omega'_b(\lambda)$ . The details of the results from model evaluation are presented in Tables S2–S4, and Table S5 for blue (494 nm), green (566 nm), red (650 nm), and NIR (790 nm) wavelength respectively. For all bands and different water types,  $\omega'_b(\lambda)$  was approximated better by the reflectance model in the SASM when compared with that in the NRP model. In comparison, the highest MARE was given by the NRP model for the green band (~75%) for water type I whereas the highest MARE of the SASM was ~4.5% in the blue band for water type V.

Since both the NRP and SASM are based on the assumption that red and NIR wavelengths are optimal for the estimation of TSS, we make a detailed comparative analysis between NRP and SASM in the red and NIR spectral regions. In the red spectral region, we find that the NRP model better estimates  $\omega'_b(\lambda)$  when CHL and CDOM are increased: MARE improved by 6.0% from type I to type VI, while for the SASM the MARE performance decreases by 0.48% from water type I to type VI. Likewise, in the NIR band, the shift in improvement over different water types is ~1.0% for the NRP model and ~0.17% for the SASM. However, comparing the red and NIR bands, the NRP model performs better for the NIR band with the MARE ~15.0% lower than the red band. For the SASM, the performance is better in the red band by ~1.0%. Illustration of the differences between the NRP model and the SASM for their performance in estimating  $\omega'_b(\lambda)$  with respect to HydroLight-modelled  $\omega'_b(\lambda)$  is shown in Figures S1a and S2a for red and NIR bands respectively for water type VI. For the variation of  $\omega'_b(\lambda)$  as a function of TSS, Figure S1b for the red band and Figure S2b for the NIR band shows that the accuracy of the estimation of  $\omega'_b(\lambda)$  decreases with increasing TSS concentration for the NRP model. The estimation of  $\omega'_b(\lambda)$  by the NRP model deviates by more than 25% for TSS

concentrations greater than 100 mg/L. The  $\omega'_b(\lambda)$  are estimated better by the SASM for the whole range of TSS when compared with the NRP for all spectral bands with maximum deviation of only 4.53% in the blue band.

**Table S2.** Comparative  $\omega'_b(494\text{ nm})$  results for the NRP and SASM models (all  $p < 0.005$ ).

Water Type	NRP			SASM		
	RMSE (sr <sup>-1</sup> )	MARE (%)	<i>r</i>	RMSE (sr <sup>-1</sup> )	MARE (%)	<i>r</i>
I	0.53	57.41	0.99	0.01	1.00	1.00
II	0.49	53.70	0.99	0.01	1.15	1.00
III	0.37	41.86	0.99	0.01	2.15	1.00
IV	0.28	32.91	0.99	0.02	2.98	1.00
V	0.23	26.00	0.99	0.02	4.53	1.00
VI	0.17	20.55	0.99	0.02	4.13	1.00

**Table S3.** Comparative  $\omega'_b(566\text{ nm})$  results for the NRP and SASM models (all  $p < 0.005$ ).

Water Type	NRP			SASM		
	RMSE (sr <sup>-1</sup> )	MARE (%)	<i>r</i>	RMSE (sr <sup>-1</sup> )	MARE (%)	<i>r</i>
I	0.83	74.71	0.98	0.02	2.08	1.00
II	0.81	73.31	0.98	0.02	2.05	1.00
III	0.73	66.86	0.98	0.02	1.92	1.00
IV	0.64	59.85	0.99	0.02	1.88	1.00
V	0.52	49.24	0.98	0.02	2.25	1.00
VI	0.45	43.06	0.98	0.02	2.66	1.00

**Table S4.** Comparative  $\omega'_b(650\text{ nm})$  results for the NRP and SASM models (all  $p < 0.005$ ).

Water Type	NRP			SASM		
	RMSE (sr <sup>-1</sup> )	MARE (%)	<i>r</i>	RMSE (sr <sup>-1</sup> )	MARE (%)	<i>r</i>
I	0.36	35.91	0.98	0.02	3.07	1.00
II	0.35	35.26	0.98	0.02	3.11	1.00
III	0.32	32.64	0.99	0.02	3.24	1.00
IV	0.29	29.62	0.99	0.02	3.44	1.00
V	0.33	33.09	0.98	0.02	3.27	1.00
VI	0.27	27.76	0.99	0.02	3.55	1.00

**Table S5.** Comparative  $\omega'_b(790\text{ nm})$  results for the NRP and SASM models (all  $p < 0.005$ ).

Water Type	NRP			SASM		
	RMSE (sr <sup>-1</sup> )	MARE (%)	<i>r</i>	RMSE (sr <sup>-1</sup> )	MARE (%)	<i>r</i>
I	0.04	21.70	0.99	0.01	4.00	1.00
II	0.04	21.57	0.99	0.01	4.00	1.00
III	0.04	20.84	0.99	0.01	3.92	1.00
IV	0.04	20.13	0.99	0.01	3.83	1.00
V	0.04	21.87	0.99	0.01	4.00	1.00
VI	0.04	20.15	0.99	0.01	3.83	1.00

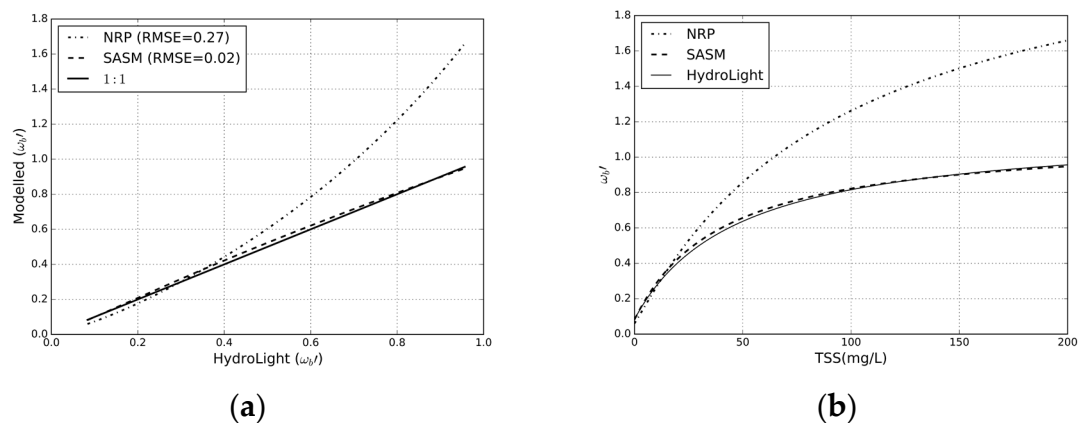


**Figure S1.** (a) Scatter plot for modelled and HydroLight  $\omega'_b(650\text{ nm})$ ; (b)  $\omega'_b(650\text{ nm})$  as a function of TSS.

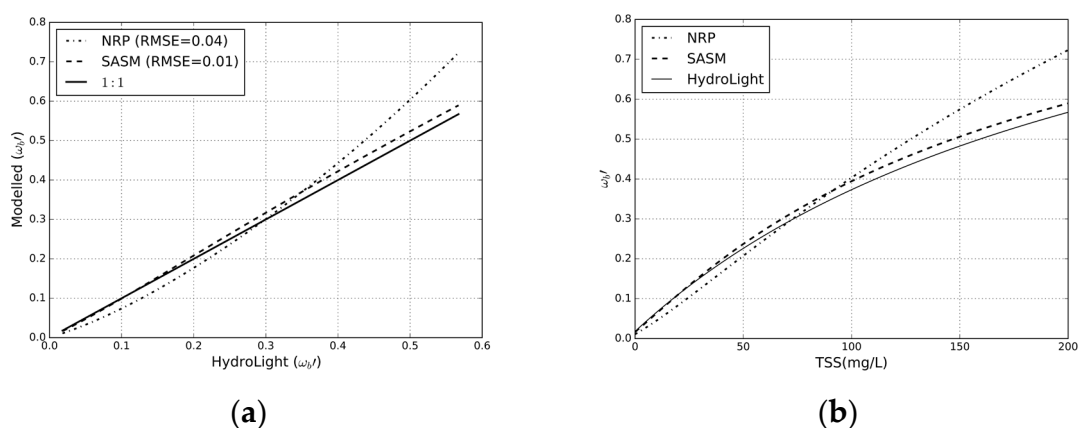


**Figure S2.** (a) Scatter plot for modelled and HydroLight  $\omega'_b(790\text{ nm})$ ; (b)  $\omega'_b(790\text{ nm})$  as a function of TSS.

## References

1. Nechad, B.; Ruddick, K.G.; Park, Y. Calibration and validation of a generic multisensor algorithm for mapping of total suspended matter in turbid waters. *Remote Sens. Environ.* **2010**, *114*, 854–866.
2. Mobley, C.; Stramski, D.; Bissett, W.P.; Boss, E.M. Optical modelling of ocean waters: Is the case 1–case 2 classification still useful? *Oceanography* **2004**, *17*, 60–67.
3. Gordon, H.R.; Brown, O.B.; Evans, R.H.; Brown, J.W.; Smith, R.C.; Baker, K.S.; Clark, D.K. A semianalytic radiance model of ocean color. *J. Geophys. Res.* **1988**, *93*, 10909–10924.
4. Lee, Z.P.; Carder, K.L.; Mobley, C.D.; Steward, R.G.; Patch, J.S. Hyperspectral remote sensing for shallow waters: 2. Deriving bottom depths and water properties by optimization. *Appl. Opt.* **1999**, *38*, 3831–3843.
5. Smith, R.C.; Baker, K.S. Optical properties of the clearest natural waters (200–800 nm). *Appl. Opt.* **1981**, *20*, 177–184.
6. Loisel, H.; Morel, A. Light scattering and chlorophyll concentration in case 1 waters: A reexamination. *Limnol. Oceanogr.* **1998**, *43*, 847–858.

